Abdominal Imaging

Published online: 12 July 2007

Abdom Imaging (2008) 33:482–488
DOI: 10.1007/s00261-007-9282-5

Imaging findings of Castleman disease of the abdomen and pelvis

L. P. Zhou,[1] B. Zhang,[2] W. J. Peng,[1] W. T. Yang,[3] Y. B. Guan,[4] K. R. Zhou[5]

[1]Department of Radiology, Cancer Hospital of Fudan University, Shanghai, 270 DongAn Road, Shanghai 200032, China
[2]Department of Radiology, Ruijin Hospital of Shanghai Jiaotong University, 197 Ruijing Er Road, Shanghai 200025, China
[3]Department of Pathology, Cancer Hospital of Fudan University, Shanghai, 270 DongAn Road, Shanghai 200032, China
[4]Department of Radiology, First Hospital of Guangzhou Medical College, 151 Yanjiang Road, Guangzhou 510120, China
[5]Department of Radiology, Zhongshan Hospital of Fudan University, Shanghai, 180 Fenglin Road, Shanghai 200032, China

Abstract

Background: The purpose of this study was to analyze the characteristic features of Castleman disease in the abdomen and pelvis as suggested by imaging findings in order to deepen the recognition and understanding of this rare disease.

Methods: A group of ten patients with pathologically proven Castleman disease in the abdomen ($n = 9$) and pelvis ($n = 1$) were included in this study. Patients were 18∼56-year-old (mean = 40); seven of them were men and three were women. Imaging findings (CT&MRI, $n = 4$; only CT, $n = 4$; only MRI, $n = 2$) were retrospectively reviewed and correlated with clinical and pathologic findings.

Results: The lesions were divided into those with localized Castleman ($n = 9$) and disseminated Castleman ($n = 1$). The pathologic subtype of all nine cases of localized disease was hyaline vascular with six patients showing a solitary mass and three having a single dominant mass surrounded by small satellite nodules. On nonenhanced CT images, the lesions were manifested as homogeneous masses of soft tissue attenuation, which was isoattenuated relative to normal muscle. On MRI, the lesions were isointense or slightly hypointense compared with that of normal muscle on T1-weighted images and hyperintense on T2-weighted images. After intravenous injection of contrast media, most of the masses (7/9) showed marked enhancement and slow washout with the degree of enhancement approaching that of the large arteries. And in the interior of four cases of larger masses (> 5 cm) was observed fissured and radial patterns in both low-density area on CT and low-signal area on MRI. These patterns were pathologically proved to be fibrous. The pathological subtype of a sole disseminated case was plasma-cell type, where imaging findings showed a lining of well defined, sharply enhanced soft-tissue nodules in retroperitoneal zone.

Conclusion: Imaging findings of Castleman disease in the abdomen and pelvis are closely related to pathological type diagnosed. The characteristic features of localized and hyaline vascular type of Castleman disease include a solitary mass or a dominant mass surrounded with small satellite nodules, and high enhancement and slow washout with the degree of enhancement approaches that of large arteries. The presence of central areas of fibrosis of the larger tumors is one of the characteristic features of this disease.

Key words: Castleman disease—Abdomen—Pelvis—Computed tomography—Magnetic resonance imaging

Castleman disease, also known as angiofollicular lymph node hyperplasia or giant lymph node hyperplasia, is a rare, usually benign process of unknown cause, characterized by lymphocyte proliferation [1–2]. Clinically, it is liable to be misdiagnosed as other hypervascular tumors by radiology and pathologic examination [3–4]. Although Castleman disease may occur anywhere along the lymphatic chain such as the neck, axilla, mesentery, thorax pancreas, spleen, adrenal, and retroperitoneum, it is described commonly located in the mediastinum, while the abdominal and pelvic Castleman disease is

Correspondence to: W. J. Peng; *email:* weijunpeng@yahoo.com

even rarer [2, 5–14]. Furthermore, the description of Castleman disease in the abdomen or pelvis in the radiology literature is mostly about CT features, while that of MRI is rare [4, 5, 8, 9, 14]. In this study, we describe the most suggesting imaging findings of ten cases of Castleman disease in the abdomen and pelvis, in which six cases had MRI data, and compared with pathological results so as to enhance the understanding of this rare disease.

Materials and methods

A retrospective review of radiological and pathological database during a 13-year period (1992–2005) revealed ten patients with Castleman disease in the abdomen or pelvis at our four institutions; seven men and three women, whose ages ranged from 18 to 56 years, with an average of 40. Of these patients, nine had localized Castleman disease and one had diffuse Castleman disease according to the description of Kim et al. [14]. Of the nine patients with localized Castleman disease, four (44%) were symptomatic, included abdominal masses ($n = 2$); abdominal pain and diarrhea ($n = 1$); epigastric discomfort and weight loss ($n = 1$). The patient with diffuse Castleman disease had general symptoms; including anemia, weight loss, fever and superficial lymphadenopathy.

Of the ten patients, four underwent both CT and MRI examinations, four CT examinations only and two MRI examinations only. For CT examinations, two patients were examined with conventional CT and six with spiral CT, with a 5–10-mm collimation and 5–10-mm intervals. For MRI examinations, all patients were examined with a 1.5-s T superconducting MR system, with 5–8 mm slice thickness and 0.5–2.0 mm gap spacing. The CT and MRI technique varied somewhat owing to the four institutions and the retrospective nature of the study; however, intravenous contrast-enhanced images had been obtained in all patients.

All lesions were independently evaluated by two radiologists aware of diagnosis for location, sizes, shape, number, internal architecture, CT density (hypodense, isodense and hyperdense), MRI signal intensity (hypointense, isointense and hyperintense) and pattern of enhancement (homogenous, overspreading, heterogeneous) and then coded by consensus. The degree of enhancement of the lesion was assessed subjectively and categorized as follows: mild, when the enhancement was similar to that of adjacent muscle; moderate, when the enhancement was higher than that of muscle but lower than that of blood vessels; high, when the enhancement was approaching that of blood vessels. Pathological manifestations were assessed to determine the pathological type of the lesion and record the non-uniformity of the tumors' internal morphology.

Results

Imaging findings

Localized type: Of the nine cases of localized Castleman disease, four were found in the mesentery, four in the retroperitoneum, and one in the left iliac fossa. Five patients presented with a large solitary mass of soft tissue attenuation, three patients presented with a dominant mass with satellite nodules, a finding suggestive of regional lymphadenopathy, and one patient presented with two large masses of soft tissue in the retroperitoneal region. All the masses were circular, oval or fusiform, well defined; with the size ranging from 3.5 to 8.0 cm. Abundant blood vessels supplying blood were also seen around the tumors in four cases (Figs. 1, 2, 3, 4).

On unenhanced CT scanning, all of the seven cases manifested as isodense mass, of which six cases were relatively homogenous; in one case, the interior of the mass had punctate calcification and low-density cystic area. All the six patients undergoing MR scans demonstrated equal signal or slightly low signal on T1-weighted images and high signal on T2-weighted images, of which three had uniform signals, in two cases the center of tumors had radial and fissured low signal on T2-weighted images while in one the center demonstrated fissured high signal on T_2WI. (Figs. 1, 2, 3).

The degree of mass enhancement varied from moderate (Figs. 4) to high (Figs. 1, 2) attenuation (moderate, $n = 2$, high, $n = 6$). The enhancement was remarkable in arterial phase, persisted in portal vein phase and delayed phase, but no enhancement was observed in a cystic necrotic area (Figs. 1, 2, 3, 4).

Of the nine localized cases, three cases demonstrated relatively homogenous enhancement in all enhanced scanning. One case demonstrated homogenous enhancement spreading from the periphery to the center. Four cases (all with masses larger than 5 cm) demonstrated early nonuniform enhancement, with the central showing radial and fissured patterns in both low density area of CT and low signal area of MRI. The delayed scan signals gradually reduced or vanished, with MRI signals more distinct than CT's. Pathological examination confirmed that they were composed of fibrous material (Figs. 1, 2, 3). One case with calcification and cystic degeneration was mixed-enhancement (Fig. 4).

Diffuse type: One case had tumors in the retroperitoneal area with manifestations of multiple soft tissue nodules of similar size of approximately 2 cm in diameter. On dynamic enhanced scan, the lesions showed marked homogenous enhancement and slow washout with density approaching that of aorta (Fig. 5). At the same time, chest CT also indicated multiple nodules resembling mediastinal lymph node enlargements.

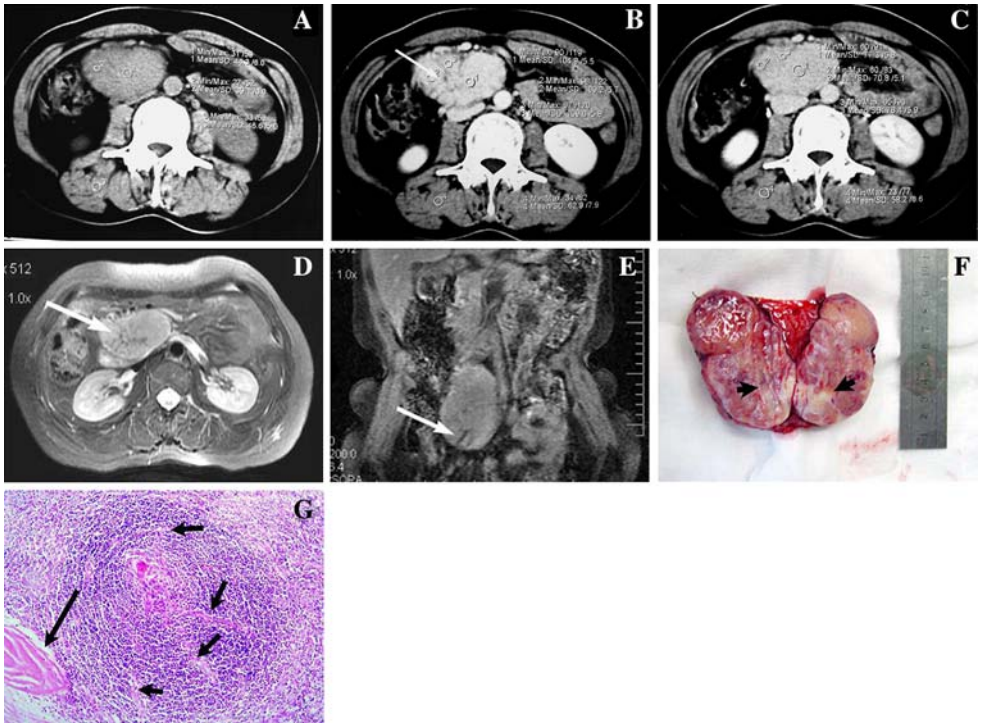

Fig. 1. Localized hyaline-vascular Castleman disease in an asymptomatic 52-year-old woman. **A** Unenhanced CT of abdomen shows a well circumscribed, oval retroperitoneal mass with homogeneous density of soft tissue. **B** Contrast-enhanced helical CT scan obtained 65 s after intravenous administration of contrast material shows distinctive enhancement of tumor with density approaching that of abdominal aorta, with visible radial enhancement low-density shadow in the center (*arrow*). **C** Delayed phase CT obtained 5 min after the intravenous administration of contrast aterial demonstrates the mass still shows higher attenuation than that of liver or back muscle and the mass appears to be homogeneous. **D** Axial T2-weighted (fast SE, 2,000/90) MR image shows a hyperintense mass with a central radial hypointense area suggesting fibrotic components (*arrow*). **E** Contrast-enhanced coronal T1-weighted (fast SE, 600/30) MR image shows an oval mass with a steaky hypointense area (*arrow*) in the lower part of it suggesting fibrotic components. **F** Photograph of a cut section of resected specimen demonstrates alternating reddish-brown and gray coloration. The *reddish-brown areas* represented cell components such as lymphatic follicles and the *gray areas* (*arrows*) represented fibrous tissue corresponding to the imaging findings. **G** The pathological section shows typical finding of hyaline-vascular Castleman disease. A great deal of small lymphocytes can be seen surrounding the tumor's center in the layers to form concentric circles. Furthermore, a great deal of hyalinized blood capillaries can be seen spreading towards the center (*short arrows*), where extensive capillary proliferation and collagen fibers (*long arrows*) are present among follicles. Hematoxylin–eosin; ×200.

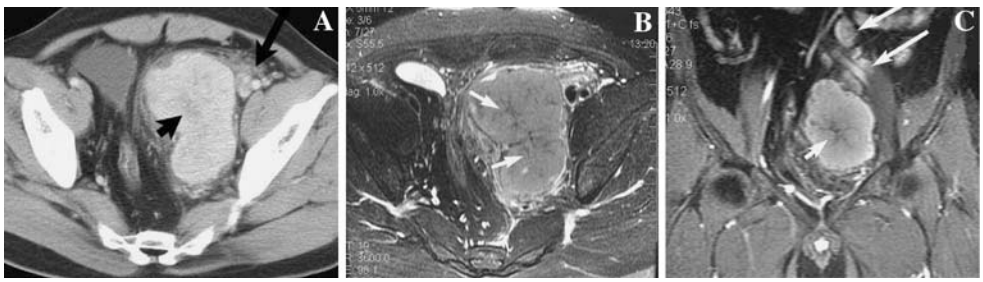

Fig. 2. A 29-year-old man with localized hyaline-vascular type of Castleman disease in the left iliac fossa appearing in dumb-bell shape. **A** Contrast-enhanced CT scan obtained 65 s after intravenous administration of contrast material shows distinctive enhancement of tumor with density approaching that of iliac artery with central area of low attenuation (*short arrow*). Note the small satellite nodules (*long arrow*) adjacent to the mass. **B** Axial T2-weighted (fast SE, 2,000/90) MR image shows a hyperintense mass with a central radial hypointense area (*short arrows*) suggesting fibrotic components that is displayed more obviously on MR T2 weighted image than on CT image. **C** Contrast-enhanced coronal T1-weighted (fast SE, 600/30) MR image shows a large mass with a central radial hypointense area (*short arrow*) suggesting fibrotic components that was confirmed by the pathology of resected specimen. Note enlarged lymph nodes (*long arrows*) represented the satellite nodules above the mass.

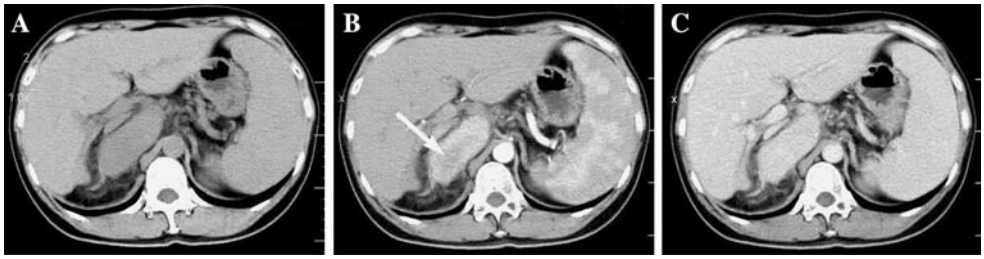

Fig. 3. Localized hyaline-vascular Castleman disease in a 42-year-old man with splenomegaly. **A** Unenhanced CT of abdomen shows a well circumscribed, homogeneous, oval right adrenal mass displacing the inferior vena cava anteriorly. **B** Contrast-enhanced CT scan obtained 25 s after intravenous administration of contrast material shows distinctive peripheral enhancement of tumor (*arrow*) with density approaching that of spleen while the center of the mass was low density. **C** Delayed phase CT obtained 70 s after the intravenous administration of contrast material shows the enhanced mass appearing to be homogeneous demonstrated a mode of enhancement distinctly progressing from the peripheral towards the center.

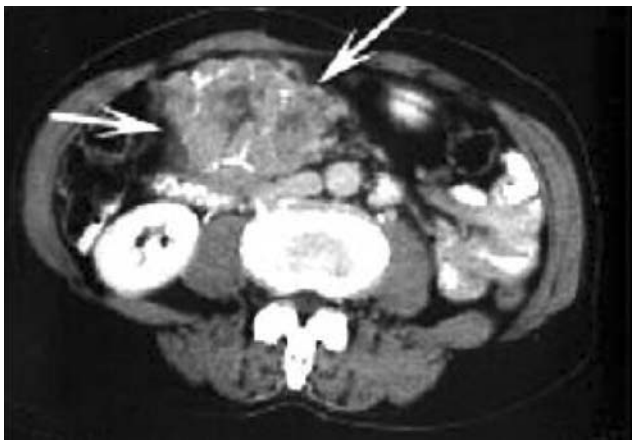

Fig. 4. An 18-year-old man with localized hyaline-vascular type of Castleman disease at the root of mesentery, demonstrating oval tumor with uneven density. Calcified focus with arborizing pattern are evident in the tumors, with necrotic area at the center (*arrows*). The delayed phase CT demonstrated moderate heterogeneous enhancement.

Fig. 5. Diffuse plasma-cell type of Castleman disease in a 42-year-old woman. Contrast-enhanced CT scan obtained 65 s after intravenous administration of contrast material shows several enlarged lymph nodes of different size in the retroperitoneal. In the delayed phase scan, the focus is persistently enhanced, with density approaching that of aorta (*arrows*).

Pathological manifestations

The foci of all the nine cases with localized Castleman disease underwent operative excision: the center of four cases revealed radial or fissured patterned regions with abundance of fibrotic components (Fig. 1F); in two abdominal cases and one pelvic case, around the main tumor and its adjacent linings were seen several satellite nodules or lymph nodes of 0.5–1.0 cm in diameter. The postoperative pathological changes were identical to those of the dominant mass. Histopathological examinations mainly indicated follicular structures disseminated in the tumors. The follicle centers underwent shrinking, and several small-hyalinized blood vessels that had thickened walls appeared. The small lymphocytes around follicles surrounded the center in laminated concentric circles resembling onionskin. Extensive blood capillary proliferation among follicular structures was observed too, thus conforming to the manifestations of hyaline vascular type of Castleman disease (Fig. 1G). The diffuse case was confirmed by aspiration biopsy. Histopathologic examinations indicated a great deal of plasma cells diffusing and infiltrating among follicles, conforming to the manifestations of plasma cell type of Castleman disease.

Discussion

Castleman disease was first reported as ''localized mediastinal lymph node hyperplasia resembling thymoma'' by Castleman in1954 [15]. For the successive cases reported afterward, the names were relatively confusing, including giant lymph node hyperplasia, hamartoma of the lymphatics, giant benign lymphoma, angiofollicular lymphadenosis, tumor-like hyperplasia of lymphoid tissue, etc.

[16]. The cause of the disease is still unknown; it might be related to chronic inflammatory reactions, drugs consumption or abnormal immunological functions.

Pathological and clinical characteristics

The main pathologic change of Castleman disease is hyperplasia of both lymphatic tissue and small blood vessels. The hallmark of this lesion was a small hyalinized and hyperplastic vascular germinal center, simulating the Hassall corpuscle of the thymus. The disease falls under three categories according to pathological changes: hyaline vascular, plasma cell and mixed-type Castleman disease. Recently, Weisenburger and McCarthy put forward the idea that Castleman disease be divided into two clinical types: localized-type and diffuse-type according to the extent of spreading of the disease [17, 18]. The two clinical types have distinct pathological and biological differences. Of the localized type, 96% were hyaline vascular type with favorable prognosis after excision of tumors. The pathology of diffuse type is mainly plasma cell type, which is mainly treated with radiotherapy, chemotherapy and immunosuppression, with poor prognosis. Castleman disease may occur in any site where lymph nodes exist. According to the literature citing statistics of 400 cases, the disease is mainly thoracic (70%), followed by the cervix (14%), abdomen (12%) and axillary region (4%) [19]. The clinical and pathological manifestations of the cases in the group used in this study were consistent with those reported in literatures.

Imaging features

Localized type: The imaging manifestations of Castleman disease are closely related to the pathological characteristics of lesions. It was reported in literatures that the enhancement of localized hyaline vascular Castleman disease was characterized by homogeneous high enhancement in the early phase of dynamic enhancement, persistent enhancement in the delayed phase, with the enhancement mode similar to that of large arteries [6, 12–14, 20]. High enhancement manifestations can be attributed first to the abundance of blood supply vessels in hyaline vascular type Castleman disease, and also focal vascular proliferation accompanied with abnormal proliferation and dilation of capillary vessels. Second, differences in the degree of enhancement may also be related to contrast agent's dosage, flow rate and mode of administration [6]. Majority of lesions (5/9) in the group had the same enhancement modes as those of Castleman disease in the abdomen and other sites reported in literatures. But in the remaining four cases (45%) with tumors larger than 5 cm, during early stage of enhancement, the interior of the tumor could be seen to have distinct radial or fissured non-enhanced areas. The non-enhancement areas were reduced or vanished in delayed scan on CT, and MRI scans of corresponding areas gave low signals on the non-enhanced T2-weighted images (Figs. 1, 2). Pathological examinations of the areas revealed abundance of parallel fibrous tissue (Fig. 1F). Thick central fibrotic bands or bundles radiating to the periphery are not uncommon in localized hyaline-vascular Castleman disease and have been described in several reports [3, 12, 14]. It might therefore indicate that in Castleman disease with relatively large tumors the manifestations of radial or fissured low signals on T2-weighted images in lesions, relatively weak enhancement or non-enhancement in early enhanced phase, can be considered to be one of the characteristic features.

One case also demonstrated a mode of enhancement distinctly progressing from the peripheral towards the center, manifested as annular enhancement with delayed scans gradually filling in. Moon et al. had observed similar enhancement manifestations in the dynamic contrast-enhanced CT exam of mediastinal Castleman disease [12, 18]. But this case had no specific pathological changes, which might reflect the lesions' differences in degree of abundance and distribution of hyaline degenerated blood vessels and fibrosis.

Another distinguishing radiological finding of localized Castleman disease was the absence or rare presence of cystic necrotic degeneration in the tumor [12–14]. This might be attributed to abundance of blood supply, good collateral circulation and low susceptibility of lymphatic follicles to necrosis. But cystic necrotic degeneration was found in the lesions of two cases (22%) in the group (Fig. 4).

Several reports demonstrated that the variety of calcification patterns as one of the features of Castleman disease which might reflect the presence calcification, in lesion's foci, of hyperplastic and calcified small blood vessels and their branches [4, 6, 12–14]. One case in our study group had a coarse calcification, disseminated in the tumor branch-wise and punctuate-wise, which was in accordance with the literatures' reports.

McAdams et al., reported that the margins of 40% lesions' foci in one group of chest cases were irregular and daughter foci could be seen, which might result in the adhesion of peripheral tissue and difficulty in excision [6]. Kim et al. also reported a single dominant mass with small satellite nodules, a finding suggestive of regional lymphadenopathy, but the pathological result was not mentioned [14]. In three cases of our study group, several daughter foci were found around the main lesion focus during operation. Imaging manifestations indicated these to have irregular or faint margins, lymphadenovarix of satellite foci around the tumors or lymphadenovarix of adjacent layers. Pathological examination also demonstrated that the lesions of daughter foci had similar characteristics as those of the main focus.

Diffuse type: It was reported in literatures that the imaging feature of the diffuse type was multiple lymph-

adenectasis demonstrated by mild to moderate enhancement, which was pathologically indicated to be mainly related to plasma cells' infiltration in large follicles and between follicles as well as scarcity of vascular proliferation [2, 14, 17, 18]. But in the group of cases reported by Kim, one case with diffuse Castleman disease of pelvis demonstrated remarkably high enhancement [14]. There is also one case of diffuse type in our study group that had remarkable enhancement of a density approaching that of abdominal aorta (Fig. 5), which was relatively exceptional, indicating that when multiple enlarged lymph nodes are remarkably enhanced, the possibility of Castleman disease should also be taken into consideration.

Differential diagnosis

Localized type: Although the imaging manifestations of localized hyaline vascular type Castleman disease possess certain characteristics features, it is liable to be misdiagnosed clinically because it is rarely seen in the abdomen and pelvis. Moreover, histological diagnosis is difficult and is essentially based on cell architecture, thus requiring study of the entire surgical specimen. And the fine-needle biopsy of a hypervascular tumor is potentially dangerous and therefore seems unadvisable [4, 21]. In fact, the possibility of this disease was taken into consideration for only three cases before operation in our study group. So the differential diagnosis of this disease by imaging exam is very important. The lesions in the abdomen and pelvis, which need to be distinguished from this type of Castleman disease in imaging include: tuberculosis of mesentery, accessory spleen, ectopic pheochromocytoma and other hypervascular lesions. Based on its imaging appearance, the most commonly stated presurgical radiologic differential diagnosis for localized Castleman disease in our series was ectopic pheochromocytoma and hypervascular sarcoma. The enhancement mode of retroperitoneal ectopic pheochromocytoma may be similar to those of localized Castleman disease. However, the signal intensity of ectopic pheochromocytoma on T2-weighted image is stronger than that of Castleman disease. The interior of the lesions revealed highly uneven density and signals accompanied by cystic central necrosis. The clinical and laboratory examinations can also contribute to the differentiation of these two diseases whereby most patients with functional ectopic pheochromocytoma show paroxysmal hypertension clinically, and in laboratory examination of urine samples show elevation of catecholamine and its metabolic product 3-methoxyl-4-hydroxyl mandelic acid. Most of localized Castleman diseases have a higher enhancement than that of hypervascular sarcoma, but if localized Castleman disease gives a moderate or a mild enhancement, it is difficult to distinguish them form hypervascular sarcoma.

Diffuse type

The diffuse and plasma cell Castleman diseases have atypical imaging manifestations and complex clinical manifestations because of extensive pathological changes and so preoperative diagnosis is still rather difficult. The distinguishing feature in imaging is mainly the lymphomas. Both types may be demonstrated by multiple lymphadenectasis with clear margins, uniform density or signal, their having moderate or mild enhancement predominantly, but necrosis is rare. Therefore, the differentiation is relatively difficult and the diagnosis is mainly dependent on pathological and immunohistochemical analysis.

In summary, imaging findings of Castleman disease in the abdomen and pelvis are closely related to pathological type diagnosed. The characteristic features of localized and hyaline vascular type of Castleman disease include a solitary mass or a dominant mass surrounded by small satellite nodules with marked enhancement and slow washout. The presence of central areas of fibrosis of the larger tumors can be helpful in the differential diagnosis of enhancing masses in the abdomen and pelvis. The diffuse type of Castleman diseases also may have marked enhancement similar to that in the large arteries.

References

1. Castleman B, Iverson L, Menendez VP (1956) Localized mediasstinal lymph node hyperplasia resembling thymoma. Cancer 9:822–830
2. Keller AR, Hochholzer L, Castleman B (1972) Hyaline vascular and plasma-cell types of giant lymph node hyperplasia of the mediastinum and other locations. Cancer 29:670–683
3. Luburich P, Nicolau C, Ayuso MC, et al. (1992) Pelvic Castleman disease: CT and MR appearance. J Comput Assist Tomogr 16:657–659
4. Irsutti M, Paul JL, Selves J, et al. (1999) Castleman disease: CT and MR imaging features of a retroperitoneal location in association with paraneoplastic pemphigus. Eur Radiol 9:1219–1221
5. Glazer M, Rao VM, Reiter D, et al. (1995) Isolated Castleman disease of the neck: MR findings. AJNR Am J Neuroradiol 16:669–671
6. McAdams HP, Rosado-de-Christensen M, Fishback NF, et al. (1998) Castleman disease of the thorax: radiologic features with clinical and histopathologic correlation. Radiology 209:221–228
7. Chaulin B, Pontais C, Laurent F, et al. (1994) Pancreatic Castleman disease: CT findings. Abdom Imaging 19:160–161
8. Taura T, Takashima S, Shakudo M, et al. (2000) Castleman's disease of the spleen: CT, MR imaging and angiographic findings. Eur J Radiol 36:11–15
9. Debatin JF, Spritzer CE, Dunnick NR (1991) Castleman disease of the adrenal gland: MR imaging features. AJR Am J Roentgenol 157:781–783
10. Johkoh T, Muller NL, Ichikado K, et al. (1998) Intrathoracic multicentric Castleman disease: CT findings in 12 patients. Radiology 209:477–481
11. Bowne WB, Lewis JJ, Filippa DA, et al. (1999) The management of unicentric and multicentric Castleman disease: a report of 16 cases and a review of the literature. Cancer 85:706–717
12. Moon WK, Im JG, Han MC (1994) Mediastinal Castleman disease: CT findings. J Comput Assist Tomogr 18:43–46
13. Meador TL, McLarney JK (2000) CT features of Castleman disease of the abdomen and pelvis. AJR Am J Roentgenol 175:115–118

14. Kim TJ, Han JK, Kim YH, et al. (2001) Castleman disease of the abdomen: imaging spectrum and clinicopathologic correlations. J Comput Assist Tomogr 25:207–214
15. Castleman B (1954) Case records of the Massachusetts General Hospital: weekly clinicopathologic exercises (case 40011). N Engl J Med 250:26–30
16. Walter JF, Rottenberg RW, Cannon WB, et al. (1978) Giant mediastinal lymph node hyperplasia (Castleman disease): angiographic and clinical features. AJR Am J Roentgenol 130:447–450
17. Weisenburger DD, Nathwani BN, Winberg CD, et al. (1985) Multicentric angiofollicular lymph node hyperplasia: a clinicopathologic study of 16 cases. Hum Pathol 16:162–172
18. McCarthy MJ, Vukelja SJ, Banks PM, et al. (1995) Angiofollicular lymph node hyperplasia (Castleman's disease). Cancer Treat Rev 21:291–310
19. Frizzera G (1985) Castleman's disease: more questions than answers. Hum Pathol 16:202–205
20. Johnson WK, Ros PR, Powers C, et al. (1994) Castleman disease mimicking an aggressive retroperitoneal neoplasm. Abdom Imaging 19:342–344
21. Rahmouni A, Golli M, Mathieu D, et al. (1992) Castleman disease mimicking liver tumor: CT and MR features. J Comput Assist Tomogr 16:699–703